

Polarized optical absorption of uv-irradiated sodium azide*

Lawrence A. Kappers, Pushpendra K. Jain, and Ralph H. Bartram

Physics Department and Institute of Materials Science, University of Connecticut, Storrs, Connecticut 06268

(Received 19 July 1976)

Optical-absorption spectra were measured for light polarized both parallel and perpendicular to the hexagonal c axis in relatively thick NaN_3 single crystals, uv irradiated at 77 K. Bands at 610 and 735 nm in perpendicular polarization have previously been attributed to F_2^+ and F centers, respectively. Bands are observed in parallel polarization at 450 and 565 nm. Isochronal pulsed anneals gave the following results: The F band at 735 nm anneals near 140 K, while the F_2^+ band at 610 nm and the 450-nm band grow larger. The 565-nm band anneals near 220 K, and the 610-nm and 450-nm bands anneal together near 260 K. A point-ion calculation for the F_2^+ center predicts $A^+ \rightarrow A^-$ and $A^+ \rightarrow B^-$ transitions, at 560 and 410 nm, which correspond with the correct polarization to the 610- and 450-nm bands, respectively. The 735-nm band and a new band at 640 nm in perpendicular polarization correspond to predicted $A^+ \rightarrow A^-$ and $A^+ \rightarrow B^-$ transitions of the F center, respectively. The 565-nm band provides evidence for a new center that was not previously suspected.

I. INTRODUCTION

The formation and bleaching of color centers in sodium azide (NaN_3) have been studied by a number of investigators,¹⁻⁶ with the object of identifying the corresponding defects and relating them to photolysis and thermal decomposition.⁷ The most extensive investigations were those of Miller and co-workers^{5,6} who correlated a near-infrared absorption band at 735 nm with a 19-line ESR spectrum previously attributed to an F center.⁸ They attributed the much more prominent optical-absorption band at 610 nm, together with its pronounced high-energy tail, to an F_2^+ center on the basis of indirect evidence, including: thermal and optical interconversion of bands; a broad ESR line correlated with the 610-nm band; a model for the production mechanism in which a double vacancy is formed preferentially by a uv photon; and a continuum-model calculation with dielectric constant adjusted to yield the correct F band (735 nm).

Sodium azide undergoes a second-order phase transition at $\sim 19^\circ\text{C}$.⁹⁻¹² Above that temperature, its crystal structure is rhombohedral ($\beta\text{-NaN}_3$) with space group D_{3d}^5 , as shown in Fig. 1.¹³ At lower temperatures, the structure is monoclinic ($\alpha\text{-NaN}_3$) with space group C_{2h}^3 ; the nature of the distortion of the pseudorhombohedral unit cell is shown in Fig. 2. Single crystals grow as thin plates with the large surfaces perpendicular to the hexagonal c axis (the z axis in Fig. 1). In the monoclinic phase, the large surfaces are perpendicular to the x axis in Fig. 2. As a consequence of this growth habit, optical absorption is most conveniently studied with light propagating parallel to the c axis and thus polarized perpendicular to it; all previously reported measurements were

performed in this fashion.¹⁻⁶

In the present work, optical-absorption spectra were measured for light polarized both parallel and perpendicular to the hexagonal c axis in relatively thick NaN_3 single crystals, uv irradiated at 77 K. The optical absorption for parallel polarization is found to differ substantially from that for perpendicular polarization. Isochronal pulsed annealing experiments were performed in order to correlate the bands in the two polarizations with one another. Some activation energies were mea-

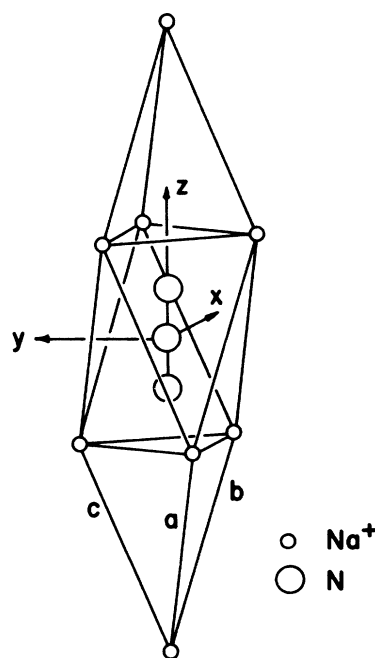


FIG. 1. Rhombohedral unit cell of $\beta\text{-NaN}_3$ (high-temperature phase).

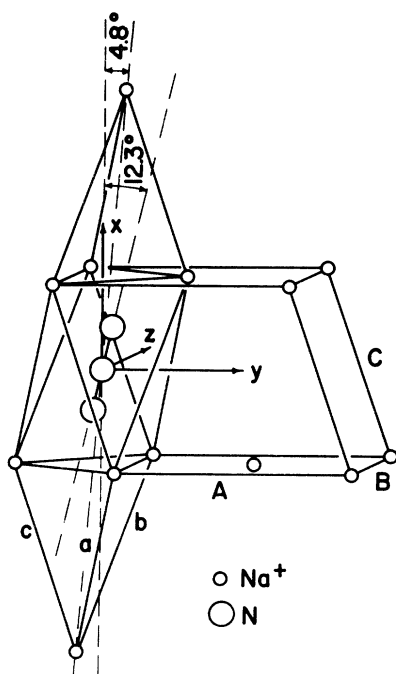


FIG. 2. Pseudorhombohedral unit cell of α - NaN_3 (low-temperature phase). Also shown are the cations associated with a conventional, face-centered-monoclinic unit cell.

sured, and additional experiments were performed on "old" crystals. These new data serve not only to test the models for color centers in NaN_3 , but also to demonstrate the existence of an additional defect.

A point-ion calculation for the F center in NaN_3 has been reported previously.¹⁴ In order to facilitate the interpretation of the new optical-absorption data, a point-ion calculation has also been performed for the F_2^+ center in NaN_3 .

The experiments are discussed in Sec. II, and the results presented in Sec. III. The point-ion calculation is described in Sec. IV, and is compared with experiment in Sec. V, which includes a discussion of all the centers.

II. EXPERIMENTAL PROCEDURES

Relatively thick single crystals of NaN_3 were obtained from J. Sharma at Picatinny Arsenal. These crystals were originally grown from solution at Fort Belvoir. Typical dimensions were $1 \text{ cm} \times 1 \text{ cm} \times 1 \text{ mm}$. The crystals were irradiated at 77 K from 2 to 5 min with an Osram 500-W mercury-vapor lamp at a distance of 10 cm using a quartz lens.

All optical-absorption measurements were made at 77 K with a Carey 14R spectrophotometer. This

double-beam instrument was modified by incorporating a matched pair of Glan-Thompson prism polarizers, which were coupled to rotate in synchronism in order to permit polarized-optical-absorption measurements over a wide range of wavelengths.

An attempt was made to detect dichroism in the plane of the crystal (polarization perpendicular to the c axis) induced by monoclinic distortion. No such dichroism was observed, presumably because of extensive twinning. In fact, the crystals depolarized the light, as was verified by means of a polarizing microscope.

Relatively thick crystals were mounted so that the beam was incident on the edge rather than the large face. With this arrangement, the light could be polarized either parallel or perpendicular to the c axis simply by rotating the Glan-Thompson prisms. Irradiation at 77 K produced coloration only in a thin layer near the surface, since NaN_3 absorbs strongly in the uv. In order to distinguish the various optical-absorption bands and to correlate them with one another, the irradiated crystals were subjected to a variety of annealing experiments, including a series of isochronal pulsed anneals. Successive anneals were performed at intervals of 20 K in the temperature range 100–280 K. The crystals were warmed quickly to the desired temperature and maintained at that temperature for 5 min. They were then returned quickly to 77 K, where spectra were recorded for both parallel and perpendicular polarizations. Pulsed annealing measurements were also made at several fixed temperatures in order to investigate decay rates of a selected absorption band.

Several experiments were performed on "old" crystals; i.e., crystals which had been previously irradiated and warmed to room temperature. Corning filters 7-51 and 7-54 were employed in conjunction with glass microscope slides in subsequent uv irradiation of these crystals at 77 K.

III. EXPERIMENTAL RESULTS

The optical-absorption spectra of α - NaN_3 after uv irradiation at 77 K are shown in Fig. 3 for light polarized both parallel and perpendicular to the c axis. The spectrum for $E \perp c$ has been reported previously by Miller and co-workers,^{5,6} who attributed the 735-nm band to F centers and the 610-nm band to F_2^+ centers, as noted above.

The qualitative changes in the optical absorption spectrum at 77 K for parallel polarization, produced by thermal annealing, are illustrated in Fig. 4. This figure reveals the existence of a single, asymmetric absorption band at 565 nm, which anneals by 240 K. It is also apparent from

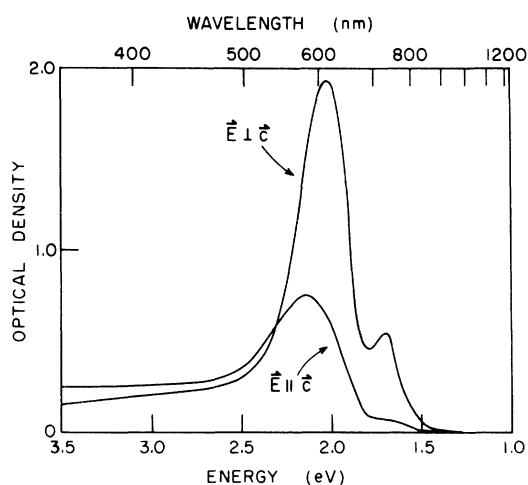


FIG. 3. Polarized-optical-absorption spectrum of NaN_3 after uv irradiation at 77 K.

Fig. 4 that a band at 450 nm is enhanced by warming to 180 K. This band, and the weaker band at 610 nm, anneal together on warming above 260 K. These features were not apparent in the spectra for perpendicular polarization.

In order to investigate these changes more systematically, we have endeavored to resolve the pulsed-annealing data into component bands. Data from different crystals were used for each polarization, with the crystal for parallel polarization more heavily irradiated, in order to insure comparable optical densities. Thus the optical density for parallel polarization is enhanced by a factor of 3.4 with respect to that for perpendicular polariza-

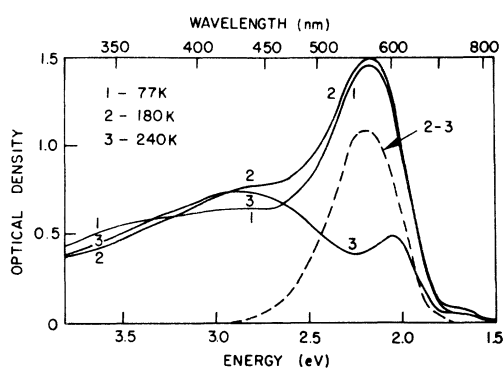


FIG. 4. Effect of annealing on optical absorption spectrum for light polarized parallel to the c axis. (5-min isochronal pulsed anneals were performed at 20-K intervals between 100 and 280 K. Spectrum 1 is produced by irradiation at 77 K, while spectra 2 and 3 correspond to maximum annealing temperatures of 180 and 240 K, respectively.) The dashed curve is the difference between spectra 2 and 3, and demonstrates the existence of an isolated band at 565 nm.

tion. (It was established that the annealing behavior is qualitatively independent of initial dose in the range of interest.) The data consist of 22 spectra in all, 11 for each polarization, corresponding to the initial uv irradiation at 77 K plus 10 annealing temperatures ranging from 100 to 280 K at 20 K intervals. Isolated bands were constructed by superposing five of these spectra, with the coefficients listed in Table I. Decomposition of the remaining spectra into combinations of these isolated bands was then accomplished by a least-squares fitting procedure. This decomposition is illustrated in Figs. 5 and 6 for the initial spectra following uv irradiation at 77 K, and is summarized for all of the bands in Table II. The resulting close fit demonstrates that to a good approximation, only five of the 22 spectra are linearly independent functions of wavelength. On the other hand, the linear transformation of the five independent spectra into isolated bands does not affect the quality of the fit, and was consequently based on other criteria. These included such obvious features as the 735- and 610-nm bands in perpendicular polarization, the 565- and 450-nm bands in parallel polarization which are evident in Fig. 4, and the nearly isotropic 340-nm band which remains at room temperature, together with consistent temperature dependence of isolated bands in both polarizations. Accordingly, the isolated bands presented here are plausible but not necessarily unique.

It is evident from the resulting decomposition that more than five optical transitions are involved, but the linear dependence of the spectra precludes meaningful decomposition into more than five isolated bands. The difficulty arises partly in distinguishing bands of the same polarization which exhibit the same annealing behavior, and partly in resolving broad overlapping bands. The former case is exemplified by the 735-nm band, which Miller and co-workers⁵ attributed to the F center.

TABLE I. Coefficients for the representation of isolated bands as linear combinations of spectra from pulsed annealing experiments. Spectra are identified by their highest annealing temperature (K) and polarization, while isolated bands are labeled by the wavelength (nm) corresponding to their maximum optical absorption. Normalization of the isolated bands is arbitrary.

Band	77 \perp	240 \perp	200 \parallel	240 \parallel	280 \parallel
735	1.009	-0.702	-0.102	0.092	-0.126
610	-0.435	1.339	-0.009	-0.149	0.073
565	0.015	-0.012	0.999	-1.005	0.045
450	-0.004	-0.218	-0.100	1.103	-0.797
340	-0.097	0.084	0.008	-0.127	1.103

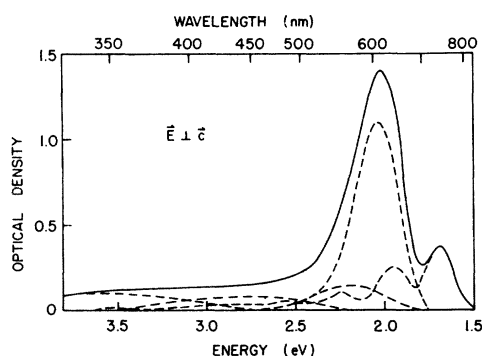


FIG. 5. Resolution of optical-absorption spectrum into isolated bands for perpendicular polarization.

We find that this band is inextricably associated with a band of comparable intensity at 640 nm, and with a long tail extending to shorter wavelength.

The amplitudes of some of the component bands, normalized to their initial amplitudes at 77 K, are plotted as a function of annealing temperature in Fig. 7. It is evident from this figure that the 735-nm band consists of two components; one which anneals near 140 K, and another which persists nearly to room temperature. Annealing of the 735-nm band is accompanied by growth of the 610- and 450-nm bands, which subsequently anneal together near 260 K. In fact, the latter two bands are always observed in the same proportion to within the accuracy of resolution of individual bands. These data suggest that the 610-nm and 450-nm bands may be transitions of the same center, identified by Miller and co-workers⁵ as the F_2^+ center. The 565-nm band, which anneals near 220 K, is clearly not associated with either the F or F_2^+ centers, and so reveals the existence of an additional defect which was previously unsuspected. The 340-nm band in perpendicular polarization is well correlated with the 735-nm band at lower temperatures, but subsequently grows as

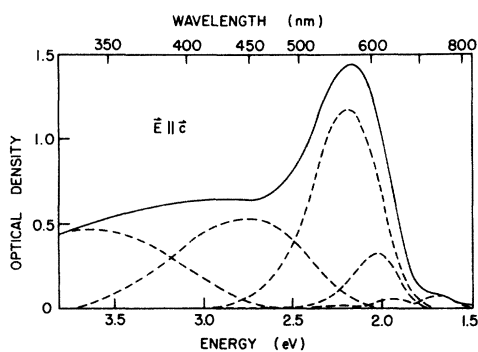


FIG. 6. Resolution of optical-absorption spectrum into isolated bands for parallel polarization.

TABLE II. Coefficients for the decomposition of pulsed annealing spectra into linear combinations of isolated bands. Spectra are identified by their highest annealing temperature (K), while isolated bands are labeled by the wavelength (nm) corresponding to their maximum optical absorption.

Spectrum	735	610	565	450	340
77 \perp	1.311	0.700	0.153	0.149	0.204
100 \perp	1.259	0.717	0.154	0.149	0.192
120 \perp	1.115	0.770	0.148	0.156	0.178
140 \perp	0.805	0.846	0.151	0.152	0.129
160 \perp	0.605	0.915	0.142	0.164	0.100
180 \perp	0.469	0.933	0.152	0.153	0.074
200 \perp	0.452	0.924	0.160	0.151	0.086
220 \perp	0.531	0.933	0.149	0.184	0.100
240 \perp	0.441	1.001	0.071	0.175	0.108
260 \perp	0.323	0.765	0.002	0.099	0.127
280 \perp	0.137	0.071	0.008	0.001	0.310
77 \parallel	0.284	0.208	1.179	0.893	0.930
100 \parallel	0.278	0.200	1.193	0.915	0.886
120 \parallel	0.251	0.213	1.205	0.984	0.862
140 \parallel	0.220	0.218	1.201	1.076	0.813
160 \parallel	0.195	0.230	1.181	1.111	0.759
180 \parallel	0.149	0.225	1.201	1.128	0.756
200 \parallel	0.162	0.231	1.127	1.134	0.777
220 \parallel	0.202	0.213	0.720	1.174	0.818
240 \parallel	0.180	0.228	0.127	1.133	0.819
260 \parallel	0.168	0.162	0.003	0.814	0.836
280 \parallel	0.101	0.010	0.015	0.122	1.005

the 610- and 450-nm bands decay. The temperature dependence of the 340-nm band is substantially different in parallel polarization, which suggests that this band is actually a composite of several unresolved broad bands. This temperature dependence is shown in Fig. 8, together with a hypothetical decomposition into component bands of the same wavelength. The 340-nm band at

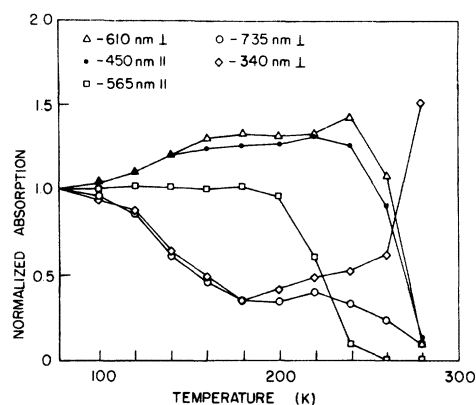


FIG. 7. Relative amplitudes of component bands as a function of annealing temperature. Amplitudes are normalized to unity at 77 K.

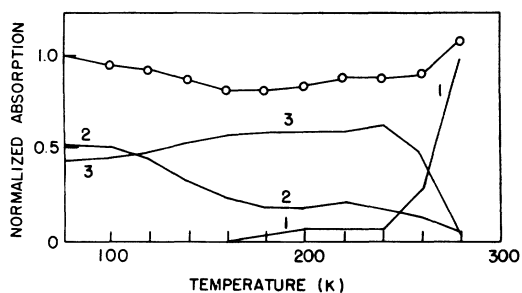


FIG. 8. Hypothetical decomposition of 340-nm band into components at the same wavelength but with different temperature dependence. Components 2 and 3 correlate with the 735- and 610-nm bands, respectively.

room temperature, which is nearly isotropic, has been associated with internal photoelectron emission from metallic sodium²; this first component grows when the F_2^+ center decays. A second component with predominantly perpendicular polarization correlates with the 735-nm band, and appears to be an ultraviolet transition of the F center. Finally, there is a third component with parallel polarization which appears to be an ultraviolet transition of the F_2^+ center. Only the first two components are observed, and in different proportions, in perpendicular polarization.

Annealing of the 565-nm band was investigated in more detail, revealing two distinct annealing stages. Annealing data for this band are presented in the following paper,¹⁵ where they are correlated with corresponding ESR data. An attempt to bleach the 565-nm band by irradiation with 565-nm light polarized parallel to the c axis was totally unsuccessful.

Miller⁶ performed several experiments on old crystals of NaN_3 ; i.e., crystals which had been warmed to room temperature after uv irradiation. He reported that the F_2^+ band (610 nm) could be reestablished by irradiation in the 340-nm band if the crystal were quickly returned to 77 K. On the other hand, if the crystal were maintained at room temperature for several hours, only the F band (735 nm) was reestablished by irradiation in the 340-nm band. Miller interpreted these results in terms of trapping of internal photoelectrons at vacancies, and breakup of double vacancies to form single vacancies at room temperature.

We have corroborated Miller's results on old crystals, and have made some additional observations. The isolated F -center spectrum produced in this fashion is essentially similar to the corresponding component spectrum shown in Fig. 5, which includes the 735- and 640-nm bands, except that it is broadened to the extent that these structural features are not well resolved. By using dif-

ferent filters, it was established that the excitation spectrum for reestablishing the F center does not coincide precisely with the 340-nm band. The effect is readily produced by wavelengths between 300 and 330 nm, while wavelengths between 330 and 400 nm are much less effective. The various color centers were produced in an old crystal by uv irradiation at 77 K, and the F center was subsequently eliminated by heating to 175 K for 10 min. It was found that irradiation in the 340-nm band reestablished the 735-nm band and enhanced the 340-nm band at the expense of the 610- and 450-nm bands. Significantly, in all of the experiments on old crystals, the 565-nm band was found to be totally unaffected by irradiation in the 340-nm band.

IV. POINT-ION CALCULATION

A point-ion calculation of the electronic structure of the F_2^+ center was performed with the objectives of testing this model for the defect, and of identifying the electronic states involved in the observed transitions. The calculation is patterned after that of Gourary and Adrian,¹⁶ but much more flexible trial functions were employed, incorporating many variational parameters.

The point-ion potential can be justified as a model pseudopotential,¹⁷ and the corresponding wave function as a pseudo-wave-function from which the true wave function can be recovered by orthogonalizing to occupied ion-core orbitals. As such, the point-ion potential is much more realistic than the continuum model assumed by Miller and co-workers,⁵ and, in particular, it preserves the correct point symmetry. In most of the present work, however, the point-ion potential was derived from the rhombohedral crystal structure ($\beta\text{-NaN}_3$) shown in Fig. 1, even though the F_2^+ center is stable only in the monoclinic phase. The higher symmetry of the defect in $\beta\text{-NaN}_3$ greatly facilitated computation, and, as shown below, the effect of monoclinic distortion is relatively slight. No attempt was made to correct for polarization and distortion¹⁸ or ion-size effects.¹⁹

The assumed structure of the defect is shown in Fig. 9. The point symmetry at the defect center is C_{2h} , the same as for the F center in $\alpha\text{-NaN}_3$ (monoclinic). Consequently, the basis functions which were employed in a prior calculation for the F center¹⁴ could be utilized for the F_2^+ center as well. These functions, which are symmetry-adapted combinations of s , p , d , and f Slater orbitals, are listed in Appendix B of Ref. 14.

The rhombohedral unit cell of $\beta\text{-NaN}_3$, shown in Fig. 1, has dimensions²⁰ $a = 5.488 \text{ \AA}$ and $\alpha = 38^\circ 43'$. In constructing the point-ion potential, the azide ion was represented by a linear array of

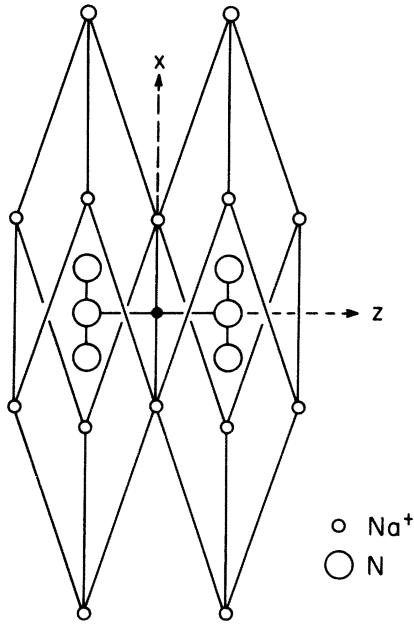


FIG. 9. Conformation of the F_2^+ center in β - NaN_3 (rhombohedral phase). The azide sites shown are vacant, and trap a single electron.

three point ions, separated by 1.17 Å, with charges of 0.714e assigned to the central ion and -0.857e assigned to each end ion.^{21,22} The point-ion potential was expanded in spherical harmonics, $Y_L^M(\theta, \phi)$, about the defect center, as indicated in Eqs. (1)–(3) of Ref. 14. The infinite-lattice sums in the expansion coefficients were evaluated by the method of Nijboer and de Wette.^{23,24} With the chosen basis set, only terms up to $L = 8$ contribute to matrix elements of the potential.

Energies of low-lying states of the F_2^+ center were calculated from the variational principle with trial functions of the form

$$\phi_n(\Gamma, \vec{r}) = \sum_m \chi_m(\Gamma; \vec{r}) C_{mn}(\Gamma), \quad (1)$$

where the $\chi_m(\Gamma; \vec{r})$ are the basis functions.¹⁴ The energies $E_n(\Gamma)$ are listed in Table III, while the corresponding optimum linear expansion coefficients $C_{mn}(\Gamma)$ and orbital exponents ζ_m are listed in Table IV.

TABLE III. Calculated energies (in rydbergs) for low-lying states of the F_2^+ center in β - NaN_3 (rhombohedral phase).

Γ	$E_1(\Gamma)$	$E_2(\Gamma)$
A^+	-0.697 08	
A^-	-0.534 82	
B^+	-0.472 47	
B^-	-0.629 76	-0.474 42

TABLE IV. Wave-function parameters for low-lying states of the F_2^+ center in β - NaN_3 (rhombohedral phase).

Γ	m	$C_{m1}(\Gamma)$	$C_{m2}(\Gamma)$	ζ_m
A^+	1	0.940 91		0.48
	2	-0.093 38		0.73
	3	0.306 03		0.63
	4	0.111 01		0.68
A^-	1	0.953 99		0.40
	2	-0.121 14		0.69
	3	0.249 92		0.64
	4	-0.112 98		0.63
B^+	1	0.994 41		0.49
	2	-0.105 58		0.44
B^-	1	0.942 56	-0.277 87	0.44
	2	0.195 36	0.855 41	0.39
	3	-0.063 60	-0.264 81	0.64
	4	-0.050 86	0.043 12	0.65
	5	0.148 31	0.054 07	0.81
	6	0.211 62	0.340 81	0.79

In the monoclinic phase (α - NaN_3), two alternative in-plane conformations of the F_2^+ center can be distinguished; these are illustrated in Fig. 10. Since one of these retains symmetry C_{2h} , it was convenient to repeat the point-ion calculation using unit-cell dimensions established by Pringle and Noakes,^{12,14} with the same basis functions. Linear expansion coefficients $C_{mn}(\Gamma)$ were optimized, but orbital exponents ζ_m were fixed at the values shown in Table IV. The changes in the energy levels $\Delta E_n(\Gamma)$ are listed in Table V, and are seen to be of the order of 1%.

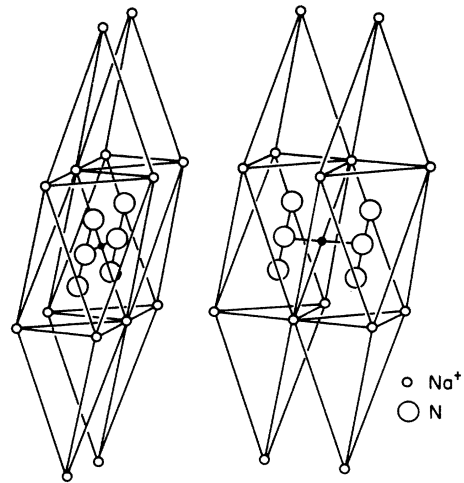


FIG. 10. Alternative conformations of F_2^+ centers in α - NaN_3 (monoclinic phase). The conformation on the left retains symmetry C_{2h} .

TABLE V. Difference in F_2^+ center energy levels (in rydbergs) between α - NaN_3 (monoclinic) and β - NaN_3 (rhombohedral).

Γ	$\Delta E_1(\Gamma)$	$\Delta E_2(\Gamma)$
A^+	+0.001 68	
A^-	+0.002 07	
B^+	+0.003 09	
B^-	+0.006 43	+0.000 83

V. DISCUSSION

The calculated energy levels and allowed transitions of the F_2^+ center are shown in Fig. 11. The $A^+ \rightarrow A^-$ transition at 2.21 eV (560 nm) and the $A^+ \rightarrow B^-$ transition at 3.03 eV (410 nm) appear to correspond with the observed 610-nm and 450-nm bands, respectively. The dashed lines in Fig. 11 show the positions of the A^- and B^- levels, relative to the A^+ level, which would give the observed transition energies. The calculated and observed transition energies agree to within 10%, which is as well as can be expected from a rigid-lattice point-ion model. The $A^+ \rightarrow A^-$ transition is strictly polarized perpendicular to the c axis, in good correspondence with the 610-nm band. The very weak 610-nm band observed in parallel polarization (with optical density reduced by a factor of 15 when corrected for unequal coloration) may be a consequence of the monoclinic structure in the low-temperature phase. The $A^+ \rightarrow B^-$ transition is allowed in either polarization, and in fact the 450-nm band is observed in both polarizations with comparable optical density.

Miller⁶ reports that the 610-nm band is actually a composite of two bands at 547 and 625 nm, which are subject to differential optical bleaching. He attributes these components to in-plane and out-of-plane vacancy pairs, respectively. A preliminary point-ion calculation for the out-of-plane F_2^+ center showed its electronic structure to be grossly incompatible with the observed spectra. We believe that Miller misinterpreted the data, which can be described more consistently in terms of a single broad band at 610 nm and the relatively narrow band at 640 nm. Thus when bleaching of F_2^+ centers is accompanied by growth of F centers, the 610-nm band decays and the 640- and 735-nm bands grow in such a manner that the optical density at 625 nm appears invariant while that at 547 nm is appreciably diminished.

When monoclinic distortion is taken into account, there are two types of in-plane vacancy pairs, as shown in Fig. 10. However, on the basis of results listed in Table V, it seems likely that their optical

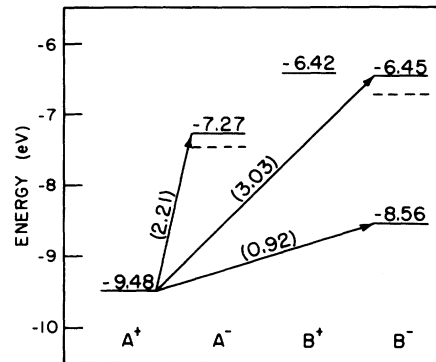


FIG. 11. Low-lying energy levels of the F_2^+ center in β - NaN_3 (rhombohedral phase). The photon energies for allowed transitions are also indicated. The dashed lines show the positions of the A^- and B^- levels, relative to the A^+ level which would correspond to the observed transitions at 610 and 450 nm, respectively.

spectra would be indistinguishable.

A comparison of the point-ion and continuum models is made in Fig. 12. It is apparent that the 610-nm band actually corresponds to a $1s\sigma_g - 2p\sigma_u$ transition in the continuum model, rather than $1s\sigma_g - 2p\pi_u$, as postulated by Miller and co-workers.⁵ In fact, the latter transition would have twice the optical density in parallel polarization as in perpendicular polarization, completely contrary to experiment. The point-ion calculation predicts a very strong crystal-field splitting of the $2p\pi_u$ level, with one component corresponding to the 450-nm band ($A^+ \rightarrow B^-$), as previously noted. Thus the continuum model would appear to be misleading.

The point-ion calculation predicts a second $A^+ \rightarrow B^-$ transition, predominantly polarized parallel to the c axis, at 0.92 eV (1350 nm). A similarly polarized infrared transition was predicted for the F center at 0.94 eV (1310 nm) in a previous calculation.¹⁴ A search for these transitions failed to yield any additional bands at energies above 0.72 eV (1750 nm). Presumably, the actual bands lie still further in the infrared.

In the case of the F_2^+ center, the data are susceptible to an alternative interpretation: It is conceivable that, as a consequence of ion-size effects, the crystal-field splitting of the $2p\pi_u$ level is actually very small, and that both $A^+ \rightarrow B^-$ transitions are associated with the 450-nm band. However, the F -center data are not susceptible to a similar interpretation. If there were no crystal-field splitting of the continuum-model $2p$ level, the F band at 735 nm would be isotropic; instead, it is found to be strongly polarized perpendicular to the c axis, as predicted by the point-ion model.¹⁴ Thus

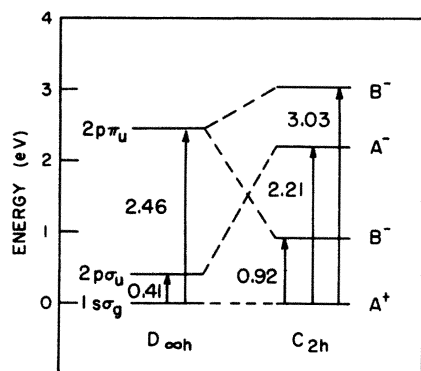


FIG. 12. Comparison of the continuum and point-ion models for the F_2^+ center in β - NaN_3 (rhombohedral phase). The continuum-model energies are from Ref. 5.

a large crystal-field splitting would appear to provide the most plausible interpretation for both centers.

Papazian⁴ observed a far-infrared absorption band at 1723 cm^{-1} which appears, from its annealing behavior, to be correlated with the 610-nm band. This infrared absorption was subsequently investigated in more detail by Bryant,²⁵ who employed NaN_3 crystals which were isotopically enriched with NaN^{15}NN , NaNN^{15}N and Na^{15}N_3 . On the basis of its observed splitting and frequency shifts, the infrared band was ultimately attributed to triangular N_3^- ,²⁶ or N_3^- ,²⁷ in D_{3h} symmetry. In an *ab initio* molecular-orbital calculation, Wright²⁸ has shown that N_3^+ has a stable secondary equilibrium in a singlet state with a cyclic conformation (D_{3h}) which lies 0.20 a.u. above the linear, asymmetric triplet ground state.²⁹ The barrier height of 0.04 a.u. (1 eV) above the cyclic state is adequate to provide the requisite stability. Peyerimhoff and Buenker,³⁰ who considered only singlet states, failed to find a stable equilibrium in the cyclic conformation of N_3^- .

It is difficult to reconcile the observed infrared absorption with an F_2^+ model for the 610- and 450-nm bands. Papazian²⁷ attributes the 610-nm band to cyclic N_3^- , instead of F_2^+ . However, correlation of the infrared and 610-nm bands in annealing does not necessarily indicate that they are transitions of the same center; instead, one center may decay by thermal ionization and the released charges may recombine at the other center. As a hypothetical example, some of the electrons released by thermal ionization of F_2^+ centers may recombine at cyclic N_3^+ centers. The remaining electrons may neutralize interstitial Na^+ ions, thus accounting for growth of the 340-nm band which has been associated with Na metal.²

The decomposition of spectra shown in Fig. 5

reveals that the F center has bands of comparable intensity at 735 nm (1.69 eV) and 640 nm (1.94 eV), both polarized perpendicular to the c axis. These bands can be readily understood from the point-ion calculation reported previously by Bartram *et al.*¹⁴ for the F center in NaN_3 . The point symmetry of the F center in β - NaN_3 is D_{3d} , and the F band corresponds to a transition from a nondegenerate A_1^+ state to a doubly degenerate E^- state with a transition energy of 2.06 eV. In α - NaN_3 , the point symmetry is reduced by monoclinic distortion to C_{2h} , and the degeneracy of the E^- level is removed; consequently two transitions are predicted, $A^+ \rightarrow A^-$ at 1.82 eV and $A^+ \rightarrow B^-$ at 1.96 eV, both polarized perpendicular to the c axis and of comparable intensity. The separation of these two bands, 0.14 eV, is somewhat less than the observed value, 0.25 eV, but it should be noted that the assumed structure of α - NaN_3 was based on x-ray measurements¹⁰ at -100°C .

If the splitting were assumed to be a linear function of temperature below 19°C , the predicted splitting at 77 K would be 0.25 eV. Thus the predictions of the point-ion calculation are in good agreement with experiment. The high-energy tail and 340-nm band associated with the F center may correspond to transitions to higher energy states which were not calculated.

Most of the 735-nm band was found to anneal near 140 K, but a residue persists nearly to room temperature, as shown in Fig. 7; this feature was also noted by Miller.⁶ Because of its relatively small optical density, it was not possible to ascertain whether this persistent residue is still associated with bands at 640 and 340 nm, although that was assumed in the decomposition of spectra. It is possible that the persistent residue is associated with F centers perturbed by other defects (analogous to F_A centers). In support of this interpretation, the residual 735-nm band is somewhat broader and less completely polarized perpendicular to the c axis than the original band. Further discussion of the residual 735-nm band, and the newly discovered 565-nm band, are deferred to the following paper,¹⁵ where correlations with ESR spectra are presented.

In summary, optical-absorption measurements for light polarized parallel to the c axis provide additional information about the electronic structure of radiation-induced defects which, together with a point-ion calculation, support the F_2^+ -center model, but refute the interpretation of its electronic structure based on a continuum-model calculation. The observed polarization and splitting of the F band supports the interpretation based on a point-ion calculation for the F center, as well. The absorption band at 565 nm, polarized parallel to

the *c* axis, reveals the presence of a new center, previously unsuspected.

ACKNOWLEDGMENTS

The authors are grateful to Dr. J. Sharma of Picatinny Arsenal, Dover, N.J., for providing

the relatively thick NaN_3 crystals on which most of the measurements were made. Thanks are also due to Professor O. R. Gilliam for providing additional crystals and to Robert Kent, Rekha Trivedi, and Gary DeLeo for help with optical-absorption measurements and data reduction.

-
- *Supported by the U. S. Army Research Office, Durham, N. C., under Grant No. DAHC 04-74-G-0234.
- ¹H. Rosenwasser, R. W. Dreyfus, and P. W. Levy, *J. Chem. Phys.* **24**, 184 (1956).
- ²J. Cunningham and F. C. Tompkins, *Proc. R. Soc. A* **251**, 27 (1959).
- ³H. G. Heal and J. P. S. Pringle, *J. Phys. Chem. Solids* **15**, 261 (1960).
- ⁴H. A. Papazian, *J. Phys. Chem. Solids* **21**, 81 (1961).
- ⁵G. J. King, B. S. Miller, F. F. Carlson, and R. C. McMillan, *J. Chem. Phys.* **35**, 1442 (1961).
- ⁶B. S. Miller, *J. Chem. Phys.* **40**, 2371 (1964).
- ⁷J. G. Dodd, *J. Chem. Phys.* **35**, 1815 (1961).
- ⁸F. F. Carlson, G. J. King, and B. S. Miller, *J. Chem. Phys.* **33**, 1266 (1960).
- ⁹B. S. Miller and G. J. King, *J. Chem. Phys.* **39**, 2779 (1963).
- ¹⁰G. E. Pringle and D. E. Noakes, *Acta Crystallogr. A* **16**, 192 (1963).
- ¹¹R. B. Parsons and A. D. Yoffe, *Acta Crystallogr.* **20**, 36 (1966).
- ¹²G. E. Pringle and D. E. Noakes, *Acta Crystallogr. B* **24**, 262 (1968).
- ¹³S. B. Hendricks and L. Pauling, *J. Am. Chem. Soc.* **47**, 2904 (1925).
- ¹⁴R. H. Bartram, P. K. Jain, and P. J. Kemmey, *Phys. Rev. B* **7**, 3878 (1973).
- ¹⁵R. H. Bartram, L. A. Kappers, and G. DeLeo, following paper, *Phys. Rev. B* **14**, 5482 (1976).
- ¹⁶B. S. Gourary and F. J. Adrian, *Phys. Rev.* **105**, 1180 (1957).
- ¹⁷B. S. Gourary and A. E. Fein, *J. Appl. Phys. Suppl.* **33**, 331 (1962).
- ¹⁸A. M. Stoneham and R. H. Bartram, *Phys. Rev. B* **2**, 3403 (1970).
- ¹⁹R. H. Bartram, A. M. Stoneham, and P. Gash, *Phys. Rev.* **176**, 1014 (1968).
- ²⁰R. W. G. Wyckoff, *Crystal Structures*, 2nd ed. (Wiley, New York, 1964), Vol. 2, p. 294.
- ²¹I. D. Campbell and C. K. Coogan, *J. Chem. Phys.* **44**, 2075 (1966).
- ²²T. Gora and P. J. Kemmey, *J. Chem. Phys.* **57**, 3579 (1972).
- ²³B. R. A. Nijboer and F. W. de Wette, *Physica (The Hague)* **23**, 309 (1957).
- ²⁴B. R. A. Nijboer and F. W. de Wette, *Physica (The Hague)* **24**, 1105 (1958).
- ²⁵J. I. Bryant, *J. Chem. Phys.* **42**, 2270 (1965).
- ²⁶J. I. Bryant, *Spectrochim. Acta* **22**, 1475 (1966).
- ²⁷H. A. Papazian, *J. Phys. Chem. Solids* **27**, 906 (1966).
- ²⁸J. S. Wright, *J. Am. Chem. Soc.* **96**, 4753 (1974).
- ²⁹T. W. Archibald and J. R. Sabin, *J. Chem. Phys.* **55**, 1821 (1971).
- ³⁰S. D. Peyerimhoff and R. J. Buenker, *J. Chem. Phys.* **47**, 1953 (1967).